JOURNAL OF Applied Polymer SCIENCE

Structures and Morphologies of *In Situ* Polymerized Blends of PMMA and ASA

Daniel Rotella Cocco, Fabiana Pires de Carvalho, Maria Isabel Felisberti
Institute of Chemistry, University of Campinas, CP 6154, 13083-970 Campinas, SP, Brazil
Correspondence to: M. I. Felisberti (E-mail: misabel@iqm.unicamp.br)

ABSTRACT: Blends of poly(methyl methacrylate), PMMA, and the elastomer ASA, a graft copolymer based on poly(acrylonitrile-*co*-styrene) (SAN) and acrylic rubber, were prepared by *in situ* polymerization and characterized according to structural, mechanical, thermal, and morphological properties. The polymerization conditions, such the presence or absence of a chain transfer agent, stirring and an inert atmosphere, influence the morphological and structural properties of the blends. In spite of the evidences of the partial miscibility between PMMA and SAN phase of the ASA, the blends are heterogeneous and present a complex morphology. The morphology of some PMMA-ASA blends is made up of an elastomeric dispersed phase in a glassy matrix, with a possible inclusion of the matrix in the elastomeric domains. The selective extraction of the blend components and infrared spectroscopy showed that cross-linking and/or grafting reactions occur on ASA chains during MMA polymerization. The syndiotacticity of PMMA obtained in the presence of ASA increases with the amount of ASA, due to possible interactions between the carbonyl groups of PMMA and the nitrile or phenyl groups of the SAN copolymer. The mechanical properties of the blends were influenced by the compositions of the blends and mainly by the conditions of polymerization. © 2013 Wiley Periodicals, Inc. J. Appl. Polym. Sci. 130: 654–664, 2013

KEYWORDS: blends; morphology; properties; characterization

Received 29 November 2012; accepted 17 February 2013; published online 2 April 2013
DOI: 10.1002/app.39188

INTRODUCTION

An effective route for obtaining new, tailor-made materials with specific and desirable properties is known generally as polymer blending.[1] Much research has been carried out on polymer blends, mainly because of the enhanced mechanical properties that these materials possess.[2] Materials that combine the excellent processing properties of thermoplastics with the elastomeric characteristics of rubbers have become technologically interesting for their use as thermoplastic elastomers (TPEs) or tough thermoplastics.[3–8] The most important commercial toughened systems is the high impact polystyrene (HIPS).[9,10] HIPS is produced by *in situ* polymerization of styrene in the presence of polybutadiene.[10]

Poly(methyl methacrylate) (PMMA) is an important polymer with a wide range of applications. However, it is a brittle material and a possible way to overcome this characteristic is the incorporation of rubber particles as toughening agent.[11–14] For this purpose Poomalai et al.[12] prepared blends of PMMA and ethylene-vinyl acetate copolymer (EVA) by melt blending, finding that the densities of the blends are lower than expected from the volume additive principle, suggesting a phase separation, micro void formation or poor interfacial adhesion between the PMMA and EVA phases. In spite of this possible shortcoming, the impact resistance increased from 19.1 to 31.96 J m^{-1} by addition of 20 wt % of EVA (~60% increase). PMMA and poly(vinyl acetate) (PVAc) blends, prepared by *in situ* polymerization by Zheng et al.,[13] exhibited a two-phase structure and the inclusion of 10 wt % PVAc resulted in a substantial thermal stabilization effect. The PMMA/PVAc blends exhibited an increase of ~150% of impact resistance with the inclusion of 5 wt % PVAc.

Chung et al.[14] synthesized blends of PMMA and poly(butyl acrylate) (PBA) rubber by seeded multi-stage polymerization. A rigid control of morphology was applied by changing the polymerization conditions. In order to prepare core/shell type polymers, the PBA core phase was firstly polymerized and then the shell phase of PMMA was polymerized onto the PBA core phase. Mixtures of MMA and BA monomers were used to prepare random copolymer particles. Gradient type particles, which present a gradual change of composition along the radial direction within the particle, were prepared using the power-feed method.[15,16] The storage modulus as a function of temperature curve shows a distinct single transition for the random copolymer. On the other hand, two well defined glass transitions for

Table I. Polymerization Conditions Used to Prepare PMMA and PMMA/ASA Blends by *In Situ* Polymerization

Method	Atmosphere	Stirring for 5 h at 60°C	Total Polymerization Time (h)	Temperature (°C)	CTA (wt %)
A	N_2	No	24	60	0.05
B	N_2	Yes	24	60	0.05
C	Air	No	192	60	0
D	N_2	Yes	24	60	0

the core/shell copolymer, which correspond to the soft and rigid homopolymers, were observed. The gradient copolymer also showed two broader transitions, due to the gradient of composition around the PBA particle. Among the blends of these three different rubber particles, those containing the gradient-type rubber particle are tougher.

In general, the blends prepared by *in situ* polymerization exhibit similar mechanical properties when compared with blends prepared by mechanical processing, however, at lower levels of the elastomeric modifier. Turchette[17] obtained blends of PMMA and poly(ethylene-*co*-propylene-*co*-diene)-*g*-poly(styrene-*co*-acrylonitrile), AES, by blending in a twin-screw mixer. PMMA is immiscible with polystyrene as well as with polyacrylonitrile (PAN), however, the blends of PMMA and SAN presents a miscibility window that depends on the molar mass of PMMA and of SAN, and especially on the acrylonitrile (AN) content in SAN.[18–25] Studies showed that the miscibility window for PMMA and SAN is between 9.5 to 34.4 wt % of AN present in the SAN.[26] Since the AN content in the SAN phase of AES is 28 wt %, at least a partial miscibility between PMMA and SAN phase of AES was expected. In fact, this hypothesis was confirmed and the SAN phase of AES acted as compatibilizer for the blend, leading to good interfacial adhesion and mechanical properties. For instance the blend containing 20 wt % of AES showed a 35% increase in impact strength compared with neat PMMA. Recently, Carvalho et al.[27,28] observed an increase of 85% in impact strength for PMMA/AES blends obtained by *in situ* polymerization and containing 14 wt % of AES.

Similar to AES, poly(acrylonitrile-*co*-styrene-*co*-butyl acrylate) or ASA is a graft copolymer of poly(acrylonitrile-*co*-styrene) (SAN) and an acrylic rubber based on poly(butyl acrylate) (PBA). ASA is obtained by *in situ* polymerization of SAN copolymer in the presence of poly(butyl acrylate). ASA is a saturated thermoplastic elastomer, which presents higher weather resistance compared with unsaturated elastomers like polybutadiene or HIPS.[29] It is widely used in the automotive industry and in appliances requiring excellent weather ability. The ASA used in this work contains 66 wt % of polystyrene (PS), 18 wt % of polyacrylonitrile (PAN) and 16 wt % of poly(butyl acrylate) (PBA), as determined by ^{13}C-NMR and contains carbon black in its formulation. The SAN component of ASA has 27% of AN, therefore, a partial miscibility between PMMA and this SAN phase is expected.

The aim of this work was the study of PMMA/ASA blends prepared by *in situ* polymerization with respect to the influence of the synthetic routes on the overall composition, the molar mass of PMMA, the grafting degree, crosslinking, morphology and mechanical and thermal properties.

EXPERIMENTAL

Proquigel Química S/A supplied methyl methacrylate monomer. BASF supplied ASA (Luran® S 778t). Methyl methacrylate (MMA) was submitted to extraction of polymerization inhibitors with a 5% NaOH aqueous solution. After this, the organic layer was washed with distilled water. The water residue was extracted with dry Na_2SO_4 and the methyl methacrylate was then distilled under vacuum and storage at −15°C in ambar flask.

To prepare PMMA/ASA blends by *in situ* polymerization of MMA, ASA was dissolved in MMA monomer under stirring during 48 h at room temperature. Polymerization was then carried out using different conditions.

Method A

Benzoyl peroxide (0.1 wt %) and 2-mercaptoethanol (0.05 wt %), as initiator and chain transfer agent (CTA), respectively, were added to the viscous and homogeneous MMA/ASA solution under stirring. After 1 h stirring at room temperature the stirring was stopped and the solution was heated to 60°C. Polymerization continued for 24 h. The full process occurred under a N_2 atmosphere.

Method B

This method differs from method A only by the fact that the stirring was maintained for 5 h after the solution reaches 60°C.

Method C

Benzoyl peroxide (0.1 wt %) was added to the viscous and homogeneous solution. The solution remained under stirring for 1 h at room temperature. The solution was heated to 60°C and remained at this temperature for 192 h without stirring under an air atmosphere.

Method D

This method differs from method B only by the absence of CTA. Table I summarizes the different conditions used for obtaining the PMMA/ASA blends. Homopolymer PMMA was also synthesized using the same conditions.

Blocks of 9 cm diameter and 10 cm height of each blends composition were obtained. A portion of the materials was milled aiming the characterization. The crushed materials were dried in a vacuum oven for 48 h at 100°C and injection molded into Izod bars (ASTM D256) using an DSM Xplore 12 mL Injection Molding machine. The barrel temperature was 230°C and the

mold temperature was kept at 60°C. At least five injection-molded specimens of each sample were submitted to impact resistance in a EMIC AIC 1 apparatus, using a 2.7 J pendulum.

The content of polyacrylonitrile in the ASA was determined from the amount of nitrogen provided by elemental analysis performed on a Perkin Elmer 2400 CHN analyzer. This same analysis was conducted on the blends to determine the actual content of the ASA.

PMMA/ASA blends prepared by in situ polymerization are not totally soluble in solvents. The insoluble fraction was gravimetrically determined after continuous and exhaustive extraction of the soluble fraction in a Soxhlet extractor. For this purpose, cellulose cartridges were dried in an air circulation oven at 100°C for 8 h. Then, samples of the blends were weighed, placed in the cartridges and subjected to extraction with chloroform for 72 h, a good solvent for all components. After this period, the cellulose cartridges containing waste material (insoluble fraction) were dried in an air circulation oven at 100°C for 8 h and then weighed.

The soluble and insoluble fractions were characterized by infrared spectroscopy in the attenuated total reflection (ATR) mode. The spectra were obtained in an Illuminati IR spectrometer manufactured by Smiths Detection equipped with a ZnSe internal reflection element (45°). The spectra were obtained under the following conditions: 64 accumulations, spectral resolution of 4 cm^{-1} and spectral range of 4000−650 cm^{-1}.

The molar mass and its distribution of the soluble fractions of the blends were determined by gel permeation chromatography (GPC) using a GPCmax Viscotek VE 2001 equipment, Viscotek VE 3580 RI Detector and Viscotek UV Dectector 2500 detectors, precolumn Viscotek TGuard 10 × 4.6 mm, three T6000M Viscotek columns, 300 × 7.8 mm with 10 μm particles, attached in series and heated to 60°C. A filtered and gas free LiBr solution (Dynamic), 10 mmol L^{-1} in DMF (Synth, distilled), was used as eluent and to prepare the solutions of the samples at 8.0 mg mL^{-1}. After filtration through PVDF 45 micrometer filters (Whatman), the samples were injected by the automated system in volumes of 100 μL, elution rate 1.0 mL min^{-1}. The calibration curve was generated by the software of the equipment, OMNISEC®, from the values of Mp patterns of injected polystyrene (PS, Viscotek, molar masses ranged from 1050 to 3,800,000 g mol^{-1}).

The thermogravimetric analysis of the blends were performed using a TA Instruments 2950 Thermogravimetric Analyzer in the temperature range from 40 to 600°C at a heating rate of 10°C min^{-1} under argon flow (100 dm^3 min^{-1}).

The ^{13}C-NMR spectra were obtained with an Inova 500 spectrometer at 125 MHz in Fourier transform mode. PMMA, ASA and the soluble fraction of the blends were dissolved in deuterated chloroform in a concentration range of 100–200 mg mL^{-1}. The ^{13}C-NMR spectra were obtained in the "inverse gated" mode which suppresses the nuclear Overhauser effect (NOE) with ^{1}H decoupled, and obtained at 25°C, with 10,000 accumulations, a pulse of 45° and 10 s timeout (delay time) between pulses, spectral width of 35,000 Hz and acquisition time of 0.965 s.

Dynamic mechanical Analyses (DMA) were performed on a DMTA V instrument from Rheometric Scientific, using the tension mode in the temperature range from −100 to 200°C, with heating rate of 2°C min^{-1}, frequency of 1 Hz and amplitude of deformation of 0.02%. The samples were cut from the central region of the blocks and from the specimen for the impact resistance test of blends in dimensions of ~6.0 mm × 3.0 mm × 1 mm.

Blend morphologies were investigated using a Carl Zeiss Libra 120 transmission electron microscope at an acceleration rate of 80 kV. The films were ultramicrotomed to obtain ultrathin sections (40 nm). Phase contrast between the blend components was achieved by exposing the samples to vapors of RuO_4 for a period of 2 h.

RESULTS AND DISCUSSION

In situ polymerized PMMA/ASA blends were prepared under different polymerization conditions aiming to study the influence of different synthesis conditions on structural, thermal, mechanical, and morphological properties of these blends.

Table II shows the compositions of the ASA/MMA solutions before polymerization and of the PMMA/ASA blends after residual monomer extraction, as well as the adopted nomenclature for the samples. For all blends, the content of ASA in the blends is higher in comparison with the initial MMA/ASA solution due to the incomplete polymerization MMA. Moreover, the ASA content in the blends produced by methods B and D is higher compared with blends obtained by methods A and C from ASA/MMA solutions of similar composition. This difference is due to the stirring, which favors the loss of the monomer to the environment, since the reaction vessel is not sealed. The yield of the synthesis of 38ASA-D blend was about 70%, lower than that observed for other blends (yields >90%). In this case the absence of the chain transfer agent is an additional factor contributing to lower polymerization yield. During the polymerization the viscosity of the reaction medium increases rapidly, decreasing the diffusion coefficient of reactive species such as macroradicals. In the presence of ASA, the change in viscosity with MMA conversion is even more drastic and dependent on the content of the elastomer in the solution. In principle, the chain transfer agent, CTA (2-mercaptoethanol in this work), has the function of molar mass control, in according the following mechanism:

$$P^{\cdot} + HO{-}(CH_2)_2{-}SH \rightarrow PH + OH{-}(CH_2)_2 - S^{\cdot}$$

$$nM + OH{-}(CH_2)_2{-}S^{\cdot} \rightarrow PS{-}(CH_2)_2{-}OH$$

where $P^{\cdot}$ is the growing polymer chain (macro radical), PH is the polymer chain with terminal H, n*M* represents the n monomer molecules and PS-$(CH_2)_2$-OH is the polymer with mercaptoethanol as terminal group. The suppression of macroradical $P^{\cdot}$ generates the "micro" radical OH-$(CH_2)_2$-$S^{\cdot}$, whose diffusion coefficient must be significantly larger than the diffusion coefficient of $P^{\cdot}$. Thus, this "micro" radical can initiate another polymer chain, increasing the polymerization yield. In the case of method C the polymerization was conducted also in absence of

Table II. Compositions of MMA/ASA Solutions and PMMA/ASA Blends; Soluble Fraction, Number Average Molar Mass $\overline{Mn}$ and Polydispersity, $\overline{Mw}/\overline{Mn}$ of the Soluble Fraction

Method	Name	ASA content (wt %)		Yield[c] (wt%)	Soluble fraction (wt%)	Soluble fraction	
		In the solution[a]	In the blend[b]			$\overline{Mn}$ (kg mol^{-1})	$\frac{\overline{Mw}}{\overline{Mn}}$
A	PMMA-A	-	-	-	-	201	1.5
	10ASA-A	6	10 ± 0.4	95	99	298	1.9
	12ASA-A	9	12 ± 0.5	96	84	410	2.4
	17ASA-A	12	17 ± 0.3	94	70	375	2.3
B	PMMA-B	-	-	-	-	232	1.6
	10ASA-B	6	10 ± 0.2	95	82	253	1.8
	14ASA-B	9	14 ± 0.5	94	72	430	2.4
	18ASA-B	12	18 ± 0.3	93	58	392	2.6
C	PMMA-C	-	-	-	-	281	2.0
	9ASA-C	6	9 ± 0.3	96	94	351	3.2
	10ASA-C	9	10 ± 0.2	98	75	305	3.5
	14ASA-C	12	14 ± 0.5	97	65	328	2.8
D	PMMA-D	-	-	-	-	362	1.9
	13ASA-D	6	13 ± 0.4	92	82	373	2.4
	15ASA-D	9	15 ± 0.3	93	68	498	2.3
	38ASA-D	12	38 ± 0.4	70	72	247	2.6

[a]ASA content before polymerization.
[b]ASA content in the blends calculated from CHN data.
[c]Calculated by from the composition of MMA/ASA and PMMA/ASA solutions.

CTA, however, the yield is equivalent to other methods in which CTA was used because the reaction time was much higher (around eight times higher).

Table II presents the soluble fraction (expressed as wt %), the number average molar mass ($\overline{Mn}$) and weighted ($\overline{Mw}$) molar masses and the polydispersity of this fraction in chloroform of the blends and of PMMA synthesized by different methods. The soluble fraction is a mixture of PMMA, ASA, and graft copolymer PMMA-*g*-ASA. A decrease in the amount of soluble fraction with increasing ASA content in the blends was observed, suggesting the occurrence of reactions between PMMA and ASA, possibly grafting followed by crosslinking. High polydispersity values and the GPC curve profiles (Figure 1) reinforce this hypothesis. The chromatograms for neat PMMA and ASA show a monomodal molar mass distribution. This is also observed for blends rich in PMMA. However, as the amount of ASA increases in the blends a shoulder around 25 min can be observed. The maximum of the peak corresponding to the chromatogram of the ASA is also around 25 min. For blends prepared by methods C and D this shoulder is more intense. These results suggest that the blends present a fraction of "free ASA" and a fraction of ASA chains grafted onto PMMA. For blends obtained in the presence of CTA the fraction of "free ASA" is smaller, which is expected since CTA increases the probability of grafting reactions involving the tertiary carbon of styrenic and acrylonitrile segments present in ASA, and the growing PMMA polymer chains. Molar mass is higher for the neat PMMA obtained by method D, in the absence of CTA, than for the neat PMMA obtained by method B in presence of CTA. The CTA controls the molar mass of polymers, "stopping" the growth of polymer chains, as discussed earlier.

The methods used to prepare the blends 12ASA-A and 14ASA-B differ from each other only by the stirring at the early hours of polymerization (method B). The stirring has an impact on the insoluble fraction, increasing it, but there is no significant variation in molar mass and polydispersity for the soluble fractions. In general, this is also true for the other blends prepared by methods A and B if the average number molar mass is taken in account. These results indicate that the stirring leads to increased exposure of the ASA to the reaction medium, favoring grafting and crosslinking reactions.

The FTIR spectra of the soluble and insoluble fraction allow the analysis of the relative composition of both. Figure 2 shows the spectra for these two fractions of the blends 15ASA-D. Both spectra show the same bands, differing only by the intensity. The bands at 2918 cm^{-1} and 2850 cm^{-1}, assigned respectively to asymmetric and symmetric stretching of the CH_2 bond of the butyl group of the poly(butyl acrylate), are observed for both fractions. However, the relative intensity of these two bands, compared with the symmetric stretching band of carbonyl group of PMMA at 1722 cm^{-1}, is higher for the insoluble fraction: $I_{C\text{-}H}/I_{C=O} = 0.13$ and 0.26 for the soluble and insoluble fractions, respectively. These results indicate that the latter fraction is richer in ASA. Similar results were observed for the other blends.

Figure 3 shows the thermogravimetric curves for PMMA, ASA and their blends obtained by the four methods. PMMA (Figure 3a) presents three stages of mass loss under an inert

Applied Polymer SCIENCE

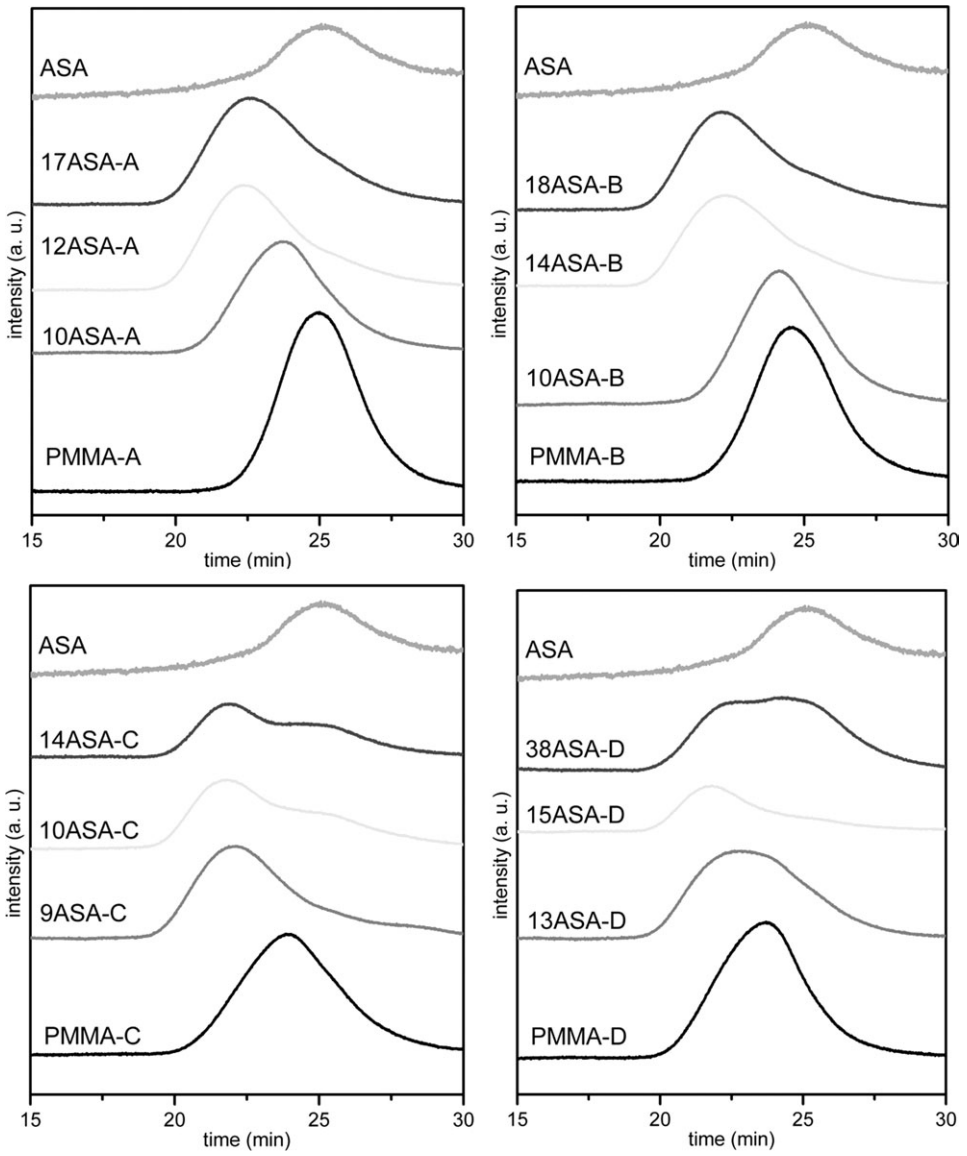

Figure 1. Gel permeation chromatograms for PMMA and its blends with ASA, obtained using the different methods.

atmosphere. According to the literature,[30–32] the first step, occurring in the range from 150°C to 250°C, is initiated by the scission of head-to-head linkages. The second step, around 300°C, is related to the scission of unsaturated chain end groups, resulting from the termination step of radical polymerization by the disproportionation mechanism involving C—C bond cleavage, β to the vinyl group. Finally, the last step occurs at temperatures between 320°C and 450°C, as a consequence of the random scission of the polymer chain. The polymerization method particularly influences the second degradation step of PMMA, as observed in Figure 3(a). The mass loss for the second step of PMMA-A and PMMA-B is almost the same; however, it is lower in comparison with the mass loss of PMMA-C and PMMA-D. This fact can be explained by the presence of CTA, which acts in the termination step of the chains, preventing the formation of unsaturated ends.

The degradation of ASA can be understood as the degradation of the SAN phase and the acrylic phase separately, however, occurring at near temperatures. The SAN phase degrades by depolymerization, leading to products of low molar mass, composed primarily of dimers, trimers, styrene, acrylonitrile, and small amounts of aromatic other compounds.[33,34] With ASA [Figure 3(a)] it is possible to observe a small mass loss at temperatures near those related to the second step of degradation of PMMA, probably related to the acrylic group, followed by the main process occurring at slightly higher temperatures than the main degradation process of PMMA. The poly(butyl acrylate) group, present in ASA, has its main stage of degradation at temperatures higher than that of PMMA,[35] coinciding with the degradation of SAN, and therefore cannot be distinguished.

Figure 3(b) shows the thermogravimetric curves for PMMA, ASA, and their blends obtained by method A and Figure 3(c) shows the thermogravimetric curves for blends with almost the same compositions obtained by different methods. The mass loss of blends starts at temperatures intermediate to the degradation of the neat components. Unlike PMMA, the blends

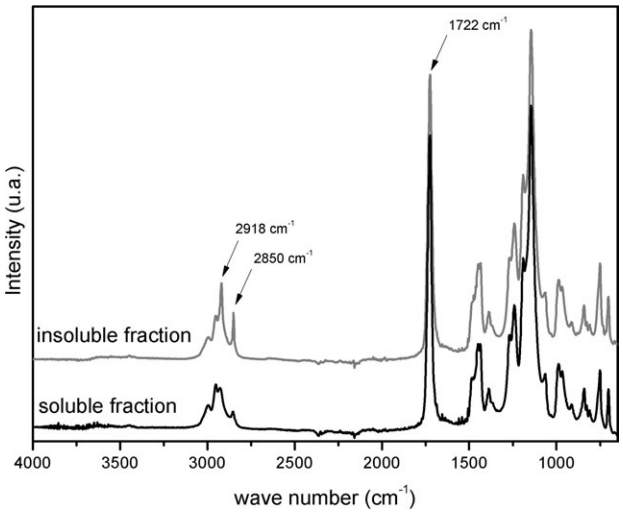

Figure 2. Infrared spectra for the soluble and insoluble fractions of the 15ASA-D blend.

basically exhibit two steps of degradation. The first around 260°C is possible related to the splitting of unsaturated ends and the second, around 350°C, is related to random scission of the main PMMA chain. The degradation step related to the scission of head-to-head linkages of PMMA chain is essentially suppressed in the blends, suggesting a lower amount of this kind of linkage in the PMMA chains.

Figure 4 shows the ^{13}C-NMR spectra and the regions corresponding to the methyl, 16.2 and 21.5 ppm (region "b"), and carbonyl, 178.5 and 176.0 ppm (region "a" highlighted in the spectra), signals for PMMA and its blends, obtained by method A. The spectra for PMMA and blends obtained by other methods are similar to these. The tacticity of neat PMMA and PMMA in the blends was evaluated through the integration of the peaks in the regions of chemical shift of methyl and carbonyl, according to the method described in the literature.[36,37] The results are summarized in Table III, showing good agreement between the data obtained considering the methyl and carbonyl signals in the ^{13}C-RMN spectra.

The PMMA obtained has predominantly syndiotactic triads (rr) and this characteristic presents the tendency of increasing as the ASA content in the blend increases. Similar results were observed and discussed for PMMA/AES blends obtained by *in situ* polymerization[27] and a possible explanation for this is the specific interactions between SAN and PMMA chains during growth.

Figures 5 and 6 show the dynamic mechanical behavior of PMMA, ASA, and PMMA/ASA blends. The storage modulus (E') curves [Figure 5(a)] for PMMA show a drop around 120°C, corresponding to the glass transition of poly(methyl methacrylate). The ASA curve shows a small drop around −30°C corresponding to the glass transition of the poly(butyl acrylate) phase and a larger drop around 120°C due the SAN phase. The storage modulus of all PMMA/ASA blends shows little decrease in the region of the poly(butyl acrylate) glass transition and a drop of two decades in the region between the PMMA and SAN glass transition, as expected for multiphase blends. Moreover, the slight decrease of the E' modulus in the temperature range corresponding to the glass transition of the rubber phase indicates that the mechanical properties of the blends are not governed by this component. This fact suggests morphology of dispersed elastomer phase [poly(butyl acrylate)] in the thermoplastic matrix constituted by PMMA and SAN, as observed earlier for the other *in situ* polymerized blends studied by our research group.[27,38,39]

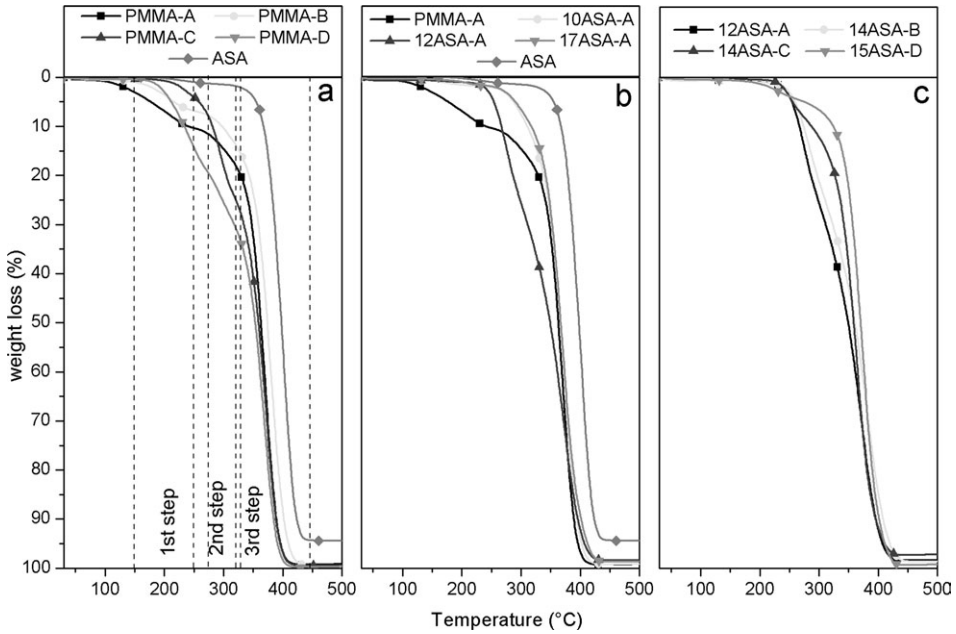

Figure 3. Thermogravimetric curves under argon atmosphere for PMMA, ASA, and their blends prepared by *in situ* polymerization using methods A, B, C, and D: (a) PMMA and ASA; (b) PMMA, ASA and the blends with different composition and prepared by method A; (c) blends with similar composition prepared by different methods.

Applied Polymer SCIENCE

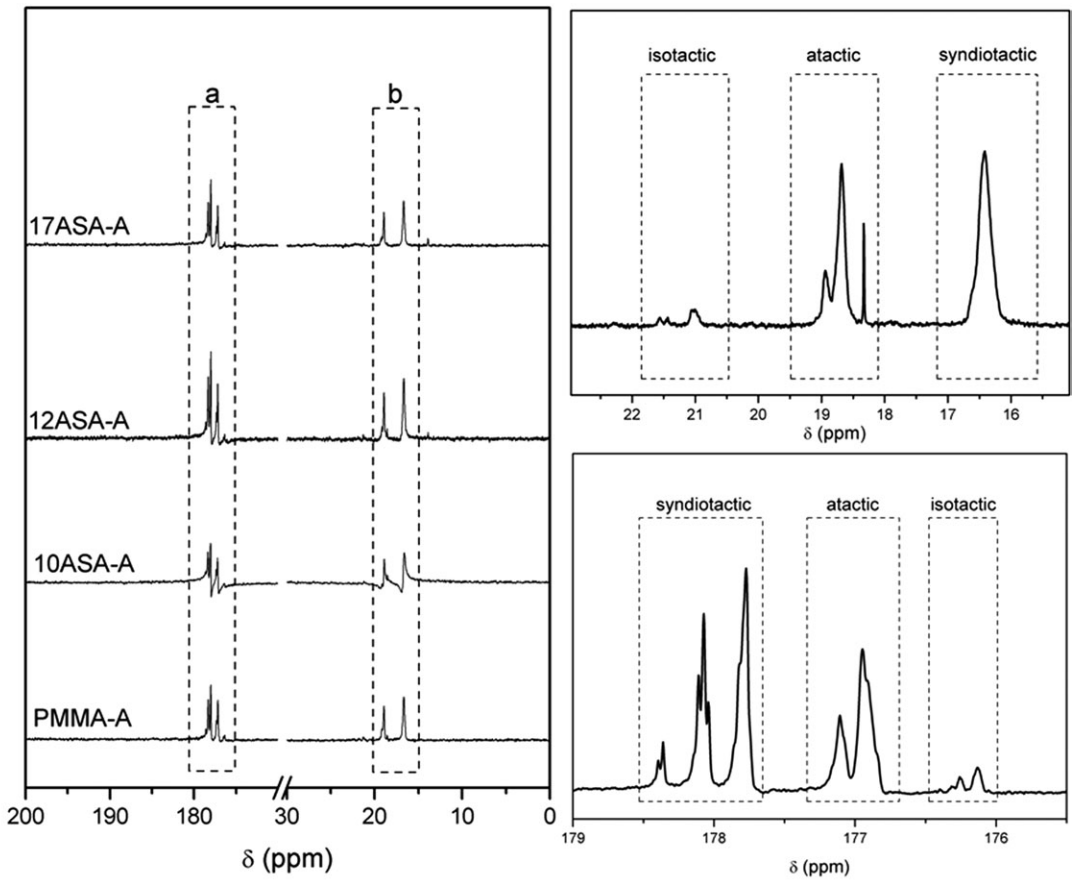

Figure 4. ^{13}C-NMR spectra for PMMA and PMMA/ASA blends. The highlighted regions "a" and "b" are the regions of the carboxyl group and methyl, respectively.

Table III. Tacticity of Pure PMMA and in the Blends Using the Carbonyl and Methyl Regions of ^{13}C-NMR Spectra

	Carbonyl region			Methyl region		
	Isotactic (%)	Atactic (%)	Syndiotactic (%)	Isotactic (%)	Atactic (%)	Syndiotactic (%)
PMMA-A	6	35	59	6	34	60
10ASA-A	5	30	65	6	28	66
12ASA-A	5	22	73	3	26	71
17ASA-A	4	23	73	3	26	71
PMMA-B	7	33	60	2	31	67
10ASA-B	5	31	64	3	34	63
14ASA-B	5	29	66	2	31	67
18ASA-B	5	26	69	3	29	68
PMMA-C	5	41	54	6	39	55
9ASA-C	3	37	60	4	41	55
10ASA-C	3	34	63	10	37	53
14ASA-C	4	36	60	2	36	62
PMMA-D	5	36	59	5	45	50
13ASA-D	4	35	61	3	47	50
15ASA-D	5	35	60	3	47	50
38ASA-D	5	32	63	9	43	48

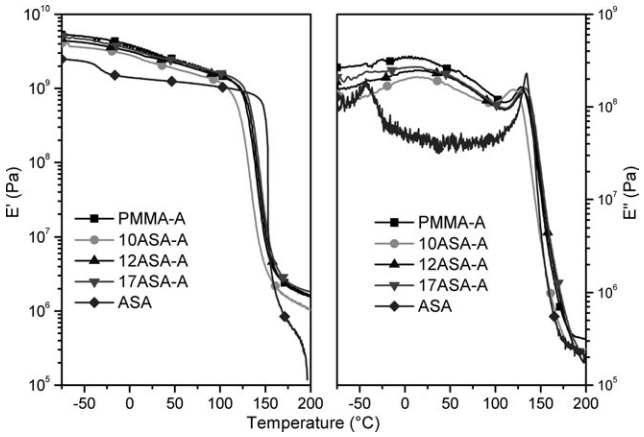

Figure 5. Storage modulus (E') and loss modulus (E'') curves as functions of temperature for PMMA, ASA and their blends obtained by methods A.

The loss modulus (E'') curves present peaks in the glass transition temperature range. The glass transition temperature (Table IV) was taken as the temperature corresponding to the maximum of the peak in the loss modulus (E'' vs. T) curves [Figures 5(b) and 6(b)].

The T_g of the PBA and SAN phase of ASA are −38°C 134°C, respectively, while for PMMA the T_g varies from 112°C to 128°C depending on their microstructure, molar mass, and polydispersity, characteristics determined by the polymerization method. As can be seen in the E'' curves for blends with similar composition [Figure 6(b)], the peaks at higher temperatures have width and position also dependent on the polymerization method. In some cases, the maximum of this peak is located between the T_g of PMMA and the SAN phase of ASA. These results suggest at least a partial miscibility between PMMA and the SAN phase of ASA.

The glass transition of the elastomer phase of the PMMA/ASA blends can not be easily observed in the E' vs. T and E'' vs. T curves due to the low concentration of poly(butyl acrylate). The glass transition of the elastomer phase of PMMA/AES[17] and

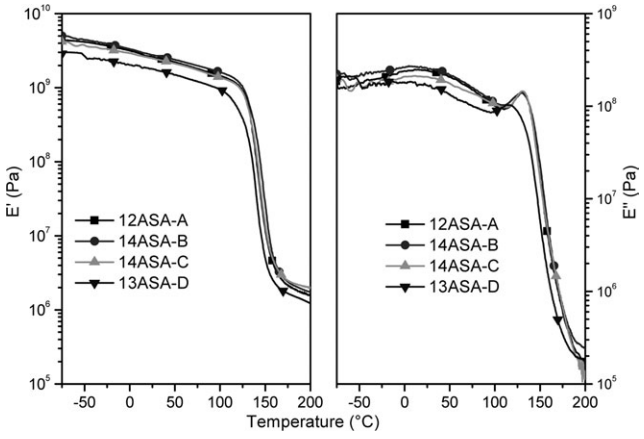

Figure 6. Storage modulus (E') and loss modulus (E'') curves as functions of temperature for PMMA/ASA blends with almost same compositions obtained by different methods.

Table IV. T_g of PMMA and SAN/PMMA Phases of the Blends and Izod Impact Strength for Injection Molded Specimens

Name	$T_{g\ SAN/PMMA}$ phase (°C)	Izod impact strength (J m^{-1})
PMMA-A	128	21 ± 2
10ASA-A	122	20 ± 3
12ASA-A	130	25 ± 1
17ASA-A	132	27 ± 2
PMMA-B	120	22 ± 2
10ASA-B	125	19 ± 2
14ASA-B	130	27 ± 2
18ASA-B	130	26 ± 2
PMMA-C	112	22 ± 2
9ASA-C	130	25 ± 2
10ASA-C	103	27 ± 2
14ASA-C	130	24 ± 2
PMMA-D	120	24 ± 2
13ASA-D	115	28 ± 2
15ASA-D	132	32 ± 2
38ASA-D	132	36 ± 4
ASA	134	147 ± 3

PHB/AES[40] blends obtained by mechanical mixing and PMMA/AES,[27,28] PS/AES,[38] and PS/EPDM *in situ* polymerized blends[39] showed a shift to lower temperature in comparison with the T_g of the same phase in AES. This is a consequence of the strong interfacial adhesion and thermal expansion coefficient difference between the dispersed phase and the matrix.[41,42] The interfacial adhesion results from the partial miscibility of SAN phase of AES and polymer matrix, what is also possible in PMMA/ASA blends.

Figure 7 shows the TEM micrograph for the ASA used in this work. ASA was stained with RuO_4, therefore the darker phase in the images is related to the SAN phase present in ASA. The micrographs show that ASA presents at least two phases distributed in a complex way: PBA within SAN macro domains dispersed in a PBA continuous phase with spreading carbon black clusters (the darker dots).

Figure 8 shows TEM micrographs for blends with similar overall compositions before and after injection molding. The blends were also stained with RuO_4. Stirring during polymerization plays a decisive role on blend morphology. While blends prepared by method B and D (with stirring) present the morphologies of dispersed phases (SAN with probable inclusions of PBA) in a matrix, the morphology of blends obtained by methods A and C (without stirring) resemble ASA morphology with macro domains of SAN containing elastomer particles dispersed in a matrix. The morphologies of the blends prepared under stirring is similar to that observed for HIPS,[43] PMMA/AES,[27,28] and PS/AES.[38] In general, the insoluble fraction is smaller for blends prepared without stirring, and the morphologies of these blends reinforce the hypothesis that the crosslinking involves ASA. If

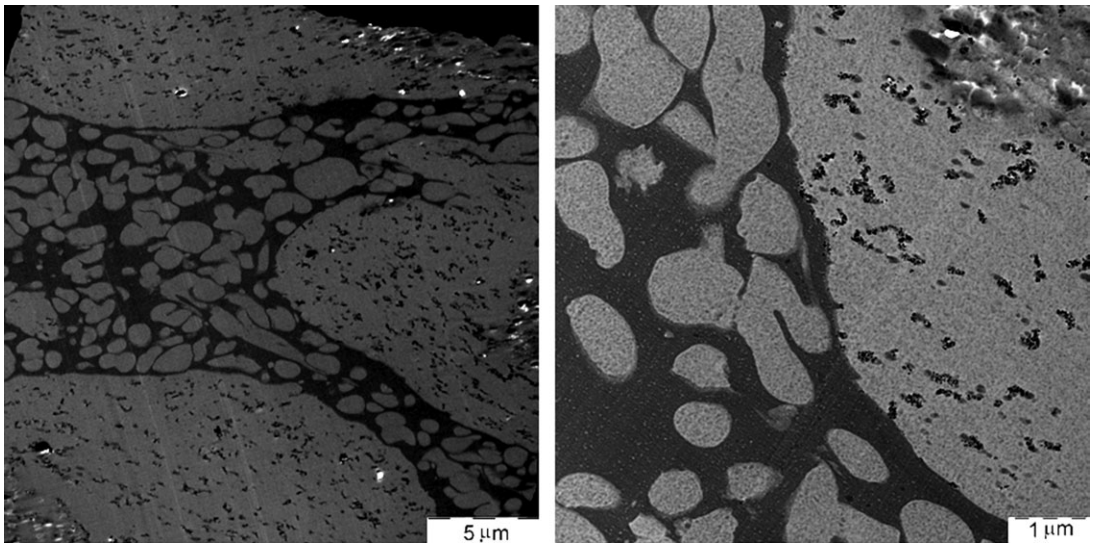

Figure 7. TEM micrographs for the neat ASA.

the morphology of ASA is partially present, then the contact between ASA and the reaction medium must be restricted.

Methods B and D differ from each other only by the presence or absence of CTA respectively. CTA influences the soluble fraction, the fraction of unsaturated end groups in PMMA chain and also molar mass and polydispersity, as discussed above. In spite of this the micrographs of the blends 14ASA-B and 15ASA-D did not differ significantly, indicating that the CTA does not cause major morphological changes. Finally, methods A and C differ by the presence of CTA and a N_2 atmosphere for the first one. Since CTA does not significantly influence the morphology, a closer look at the blends 12ASA-A and 14ASA-C shows that the atmosphere also does not have an important influence on the morphology. These blend micrographs show almost the same behavior, with blend 14ASA-C showing an apparently more defined interface between the SAN phase and the matrix. It is worth noting that the blend 14ASA-C was obtained after 192 h of polymerization, so this definition of the interface can be related to a kinetic factor.

After the injection process, the 12ASA-A-i blend presents morphological changes, seemingly an inversion of phases. The blends 14ASA-B-i and 15ASA-D-i show the same behavior after injection. The spherical domains deform toward the injection flow and are better distributed in the matrix. The 14ASA-C-i blend does not show significant changes in morphology. Comparing the morphological changes caused by the injection process, the blends obtained under stirring during the polymerization show no significant changes. This can be attributed to a decrease in interfacial tension between the matrix and dispersed phase caused by agitation and consequent grafting. Therefore, under the high temperature and shear of the injection process, the blends obtained by methods B and D do not undergo major changes, as observed for the blend 12ASA-A-i. As for the blend 14ASA-C-i, the kinetic factors already mentioned may be responsible for not causing morphological changes after injection.

Table IV presents the Izod impact strength for PMMA, ASA, and their injection molded blends. PMMA is a brittle material that has low impact resistance (about 22 J m^{-1}). The blends show a tendency to increase the impact resistance compared to PMMA. This behavior is consistent with that suggested by the SEM micrographs. The greatest increase in impact strength is observed for the blend was 38ASA-D-I, containing 38 wt % (36 $\pm$ 4 J m^{-1}), representing a 50% increase. This increase is modest, since the rubber content in the ASA is 16%, so a blend with 38% of ASA actually contains only 6% rubber.

CONCLUSIONS

The *in situ* polymerization of MMA in the presence of ASA resulted in a complex mixture whose structural and morphological characteristics are influenced by the conditions of preparation. The choice of preparation conditions, such as presence or absence of a chain transfer agent, stirring, percentage of elastomer, and atmosphere is crucial for the properties of these blends. Blends of PMMA/ASA obtained by *in situ* polymerization have intermediate thermal stability compared to the pure components. The increase in ASA content in the solution of MMA influences the tacticity of PMMA in the blend, suggesting an interaction between ASA and poly(methyl methacrylate). The results of dynamic mechanical analysis, suggest at least partial miscibility between the SAN phase of ASA and PMMA, resulting in good interfacial adhesion between the elastomer phase in a matrix of PMMA/SAN. The SEM micrographs of cryogenic fractures of PMMA and the blends suggest a toughened system, what could be verified by impact resistance test, reaching a 50% increase in impact strength. Blends obtained by method D reach a more pronounced increase, possibly due to better dispersion of the elastomeric phase in the matrix of PMMA/SAN caused

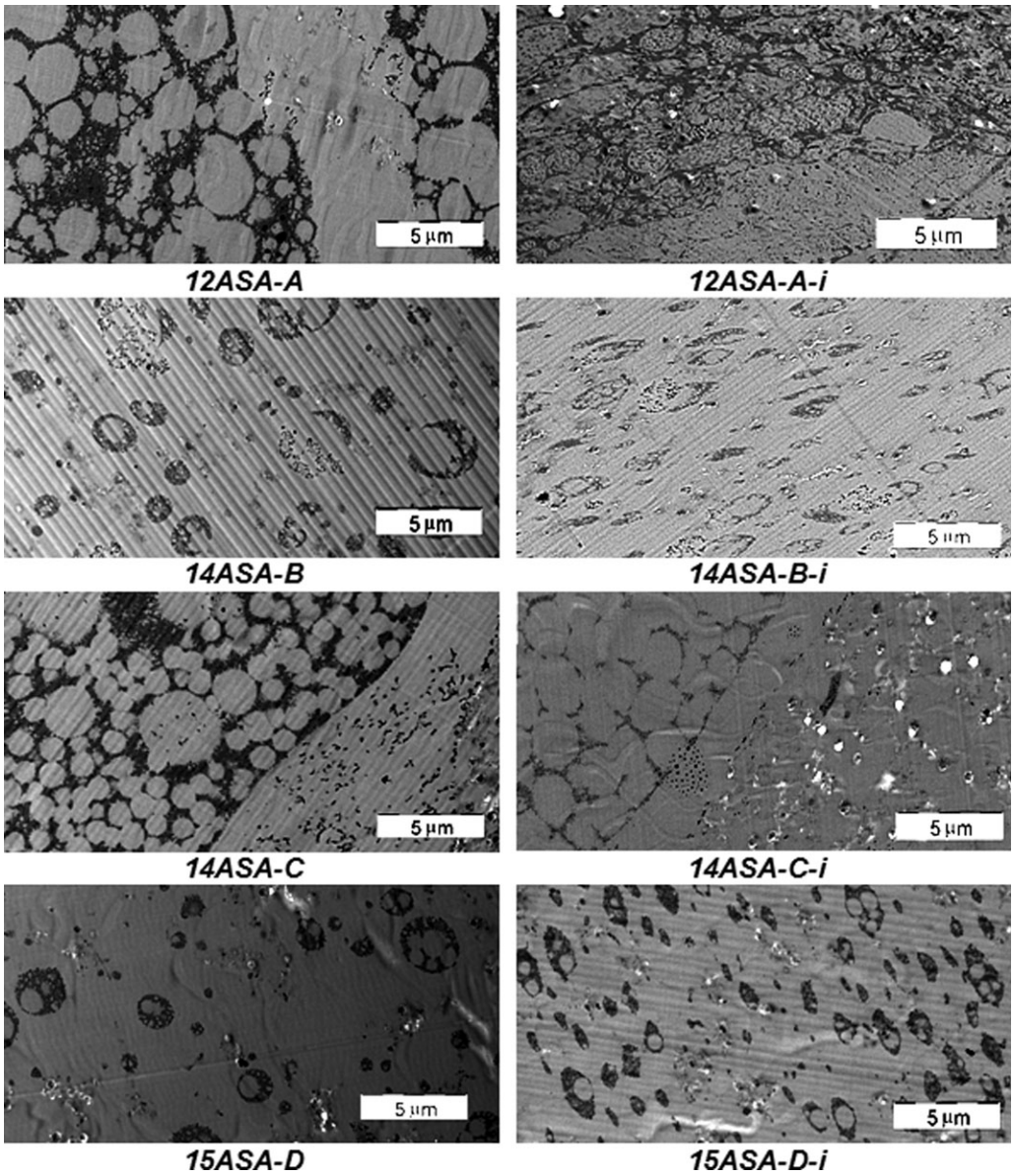

Figure 8. TEM micrographs for the blends before and after the injection process.

by stirring during the polymerization and the higher molar mass (due to the absence of chain transfer agent).

ACKNOWLEDGMENTS

The authors would like to thank Prof. C.H. Collins for manuscript revision and CNPq, FAPESP (2010/02098-4 and 2010/17804-7), Petrobras and IQ-UNICAMP for financial support.

REFERENCES

1. Dong, J.; Zonglin, L.; Feng, Y.; Zheng, C. *J. Appl. Polym. Sci.* **2006**, *100*, 1547.
2. Dong, J.; Liu, Z.; Han, N., Wang, Q., Xia, Y. J. *J. Appl. Polym. Sci.* **2004**, *92*, 3542.
3. Yoo, Y.; Cui, L.; Yoon, P. J.; Paul, D. R. *Macromolecules* **2010**, *43*, 615.
4. Shamsuri, A. A.; Daik, R.; Ahmad, I.; Jumali, M. H. H. *J. Polym. Res.* **2009**, *16*, 381.
5. Axtell, F. H.; Autsawasatain, D.; Rujiranontapong, K. *Plast. Rubber Process. Appl.* **1992**, *18*, 47.
6. Ohishi, H.; Ikehara, T.; Nishi, T. *J. Appl. Polym. Sci.* **2001**, *80*, 2347.
7. Ramsteiner, F.; Heckmann, W.; MacKee, G. E.; Breulmann, M. *Polymer* **2002**, *43*, 5995.
8. Thiraphattaraphun, L.; Kiatkamjornwong, S.; Prasassarakich, P.; Damronglerd, S. *J. Appl. Polym. Sci.* **2001**, *81*, 428.
9. Hwang, I. J.; Lee, M. H.; Kim, B. K. *Eur. Polym. J.* **1998**, *34*, 671.
10. Tanabe, T.; Furukawa, H.; Okada, M. *Polymer* **2003**, *44*, 4765.
11. Wrotecki, C.; Heim, P.; Gaillard, P. *Polym. Eng. Sci* **1991**, *31*, 213.

12. Poomalai, P.; Ramaraj, B.; Siddaramaiah. *J. Appl. Polym. Sci.* **2007**, *104*, 3145.
13. Zheng, S.; Huang, J.; Li, J.; Guo, Q. *J. Appl. Polym. Sci.* **1998**, *69*, 675.
14. Chung, J.-S.; Choi, K.-R.; Wu, J.-P.; Han, C.-S.; Lee, C.-H. *Korea Polym. J.* **2001**, *9*, 122.
15. Bassett, D. R.; Hoy, K. L. In Emulsion Polymers and Emulsion Polymerization; Bassett, D. R.; Hamielec, A. E., Eds.; ACS Symposium Series *164*; American Chemical Society: Washington, DC, **1981**; p 371.
16. Choi, S. B.; Jang, T. H.; Yoo, J. N.; Lee, C. H.(LG Cehmical Ltd.) U.S. Patent 5,618,888 (**1997**).
17. Turchette, R. Blendas de PMMA e AES: Morfologia e Propriedades Mecânicas. Master Thesis, University of Campinas, Campinas, Brazil, December **2002**
18. Fowler, M. E.; Paul, D. R.; Barlow, J. W. *Polymer* **1987**, *28*, 1177.
19. Feng, H.; Feng, Z.; Ye, C. *Polym. J.* **1996**, *28*, 661.
20. Naito, K.; Johnson, G. E.; Allara, D. L.; Kwei, T. K. *Macromolecules* **1979**, *11*, 1260.
21. Madbouly, S. A.; Ougizawa, T.; Inoue, T. *Macromolecules* **1999**, *32*, 5631.
22. Zheng, S.; Li, J.; Guo, Q.; Mi, Y. *J. Mater. Sci.* **1997**, *32*, 3463.
23. Suess, M.; Kressler, J. K.; Kammer, H. W. *Polymer* **1987**, *28*, 957.
24. Jo, W. H.; Kim, H. C.; Baik, D. H. *Macromolecules* **1991**, *24*, 2231.
25. Hiroshi, H.; Shigeki, T.; Kunihiko, T. *J. Appl. Polym. Sci.* **1998**, *70*, 2515.
26. Kashiwagi, T.; Inaba, A.; Brown, J. E.; Hatada, K.; Kitayama, T.; Masuda, E. *Macromolecules* **1986**, *19*, 2160.
27. Carvalho, F. P.; Gonçalves, M. C.; Felisberti, M. I. *Macromol. Symp* **2010**, *96*, 596.
28. Carvalho, F. P.; Gonçalves, M. C.; Felisberti, M. I. *J. Appl. Polym. Sci.* **2012**, *124*, 2846.
29. Saron, C.; Felisberti, M. I. *Mater. Sci. Eng. A* **2004**, *370*, 293.
30. Peterson, J. D.; Vyazovkin, S.; Wight, A. *J. Phys. Chem. B* **1999**, *103*, 8087.
31. McCaffrey, V. P.; Harbron, E. J.; Forbes, M. D. E. *J. Phys. Chem. B* **2005**, *109*, 10686.
32. Chang, T. C.; Liao, C. L.; Wu, K. H.; Chiu, Y. S. *Polym. Degrad. Stab.* **1999**, *64*, 127.
33. Chiantore, O.; Guaita, M.; Lazzari, M.; Ravanetti, G. P. *Polym. Degrad. Stab.* **1995**, *47*, 141.
34. Chiantore, O.; Trossarelli, L.; Lazzari, M. *Polymer* **1998**, *39*, 2777.
35. Konaganti, V. K.; Madras, G. *Polym. Degrad. Stab.* **2009**, *94*, 1325.
36. Ferguson, R. C.; Ovenall, D. W. *Macromolecules* **1987**, *20*, 1245.
37. Delgado, A. R.; Mariott, W. R.; Chen, E. Y. X. *Macromolecules* **2004**, *37*, 3092.
38. Lourenço, E.; Felisberti, M. I. *Eur. Polym. J.* **2006**, *42*, 2632.
39. Lourenço, E.; Gonçalves, M. C.; Felisberti, M. I. *J. Appl. Polym. Sci* **2009**, *112*, 2638.
40. Carvalho, F. P.; Quental, A. C.; Felisberti, M. I. *J. Appl. Polym. Sci* **2008**, *110*, 880.
41. Larocca, N. M.; Hage, E. Jr; Pessan, L. A. *Polymer* **2004**, *45*, 5265.
42. Bates, F. B.; Cohen, R. E.; Argon, A. S. *Macromolecules* **1982**, *16*, 1108.
43. Grassi, V. G.; Forte, M. M. C.; Dal Pizzol, M. F. *Polímeros* **2001**, *11*, 158.